

1 Title: In Need of Age-Appropriate Cardiac Models: Impact of Cell Age on Extracellular Matrix  
2 Therapy Outcomes

3 Short Title: Cell Age Effect on ECM Therapy Outcomes

4 Authors: S. Gulberk Ozcebe<sup>1</sup>, Pinar Zorlutuna<sup>1,2,3</sup>

5 <sup>1</sup> Bioengineering Graduate Program, University of Notre Dame, Notre Dame, IN, 46556, USA

6 <sup>2</sup> Department of Aerospace and Mechanical Engineering, University of Notre Dame, Notre  
7 Dame, IN, 46556, USA

8 <sup>3</sup> Harper Cancer Research Institute, University of Notre Dame, Notre Dame, 46556, USA

9

10 Author Contributions: S.G.O. and P.Z. designed research, S.G.O. performed research,  
11 analyzed data, S.G.O. and P.Z. conducted review and editing, P.Z. provided funding, project  
12 administration, and resources, S.G.O. wrote the paper and P.Z. revised the paper.

13

14 Corresponding Author:

15 Pinar Zorlutuna, pzorlutuna@nd.edu

16

17 Competing Interests Statement: The authors have no competing interest to disclose.

18 Ethics Statement: Deidentified human hearts were collected through the Indiana Donor  
19 Network under the Institutional Review Board (IRB) approval for deceased donor tissue  
20 recovery. All human tissue collection conformed to the Declaration of Helsinki.

21 Data availability statement: The raw/processed data required to reproduce these findings  
22 can be shared upon reasonable request.

23

24

25

26

27

28

29 Keywords: Aging, extracellular matrix therapies, gene expression, human iPSC-derived  
30 cardiomyocytes, cellular aging, cytokines, cardiac declines with age, human heart

31

## 32 **ABSTRACT**

33 Aging is the main risk factor for cardiovascular disease (CVD). As the world's population ages  
34 rapidly and CVD rates rise, there is a growing need for physiologically relevant models of  
35 aging hearts to better understand cardiac aging. Translational research relies heavily on  
36 young animal models, however, these models correspond to early ages in human life,  
37 therefore cannot fully capture the pathophysiology of age-related CVD. Here, we  
38 chronologically aged human induced pluripotent stem cell-derived cardiomyocytes (iCMs)  
39 and compared in vitro iCM aging to native human cardiac tissue aging. We showed that 14-  
40 month-old advanced aged iCMs had an aging profile similar to the aged human heart and  
41 recapitulated age-related disease hallmarks. We then used aged iCMs to study the effect of  
42 cell age on the young extracellular matrix (ECM) therapy, an emerging approach for  
43 myocardial infarction (MI) treatment and prevention. Young ECM decreased oxidative stress,  
44 improved survival, and post-MI beating in aged iCMs. In the absence of stress, young ECM  
45 improved beating and reversed aging-associated expressions in 3-month-old iCMs while  
46 causing the opposite effect on 14-month-old iCMs. The same young ECM treatment  
47 surprisingly increased SASP and impaired beating in advanced aged iCMs. Overall, we  
48 showed that young ECM therapy had a positive effect on post-MI recovery, however, cell age  
49 was determinant in the treatment outcomes without any stress conditions. Therefore, "one-  
50 size-fits-all" approaches to ECM treatments fail, and cardiac tissue engineered models with  
51 age-matched human iCMs are valuable in translational basic research for determining the  
52 appropriate treatment, particularly for the elderly.

## 53 **1. INTRODUCTION**

54 Age is a significant risk factor for cardiovascular diseases (CVD), including myocardial  
55 infarction (MI). Studies show that more than half of CVD morbidity and long-term mortality  
56 following MI occur in individuals aged 65 years and older [1,2]. Age-related changes at the  
57 cellular, extracellular, and tissue levels negatively impact disease diagnosis as well as  
58 therapeutic outcomes. Pharmacological treatment outcomes were reported to be  
59 inconsistent and unpredictable for the elderly [3]. Similarly, despite the demonstrated  
60 benefits of cell-based therapies for MI in preclinical studies, early clinical trials resulted in  
61 limited improvement in left ventricular ejection fraction and ventricular remodeling,  
62 particularly for the elderly [4]. This is mainly due to decreased responsiveness of aged cells  
63 to their environment, and consequently to treatments [5,6]. Understanding cardiac aging  
64 and the effect that this has on CVD therapy outcomes are essential to ultimately prevent and  
65 treat age-associated disease syndromes.

66 Decellularized extracellular matrix (ECM) is a promising biomaterial for the regeneration  
67 and repair of musculoskeletal[7], neural[8], liver[9], and cardiovascular systems [10,11].  
68 Studies have reported regenerative capabilities to be more effective when ECM was obtained  
69 from young tissues[6,12]. We previously showed the differences in the human induced  
70 pluripotent stem cell (iPSC)-derived cardiomyocytes (iCM) response to young, adult, and aged  
71 cardiac ECM. We showed that young ECM increases cell proliferation and drug  
72 responsiveness, improves cardiac function overall, initiates cell cycle re-entry, and mitigates

73 oxidative stress damage in quiescent state aged iCMs [6]. Moreover, regardless of the ECM  
74 age, other groups have demonstrated the feasibility of using ECM for post-MI ventricular  
75 remodeling and cardiac functional recovery (i.e., LVEF) in animal models. Porcine cardiac  
76 ECM-derived hydrogels have been reported to increase the number of endogenous  
77 cardiomyocytes while preserving post-MI cardiac function[13]. Neonatal mouse cardiac ECM  
78 was shown to be more effective to prevent post-MI adverse ventricular remodeling, such as  
79 fibrosis, compared to adult ECM[14]. In another study, zebrafish heart ECM, which is known  
80 to be highly regenerative, was reported to exert pro-proliferative effects and contribute to  
81 post-MI cardiac regeneration in adult mice[15]. A recent clinical study showed that hydrogels  
82 derived from decellularized porcine myocardium improved left ventricular function in post-  
83 MI patients (57 to 62-year-old) [16]. Taken together, these studies provided valuable  
84 information on the safety, feasibility, and efficacy of ECM as a regenerative and post-MI  
85 therapy. There is a growing trend towards using ECM therapies, alone or in combination with  
86 cells, for MI. However, because current studies are largely based on young cells and young  
87 animal models, we still have a limited understanding of how the aged heart would respond  
88 to ECM therapies. As MI disproportionately affects the elderly, and the therapy outcomes  
89 vary with the patient age, here we generated an age-appropriate heart tissue model using  
90 aged iCMs and investigated ECM therapies for both MI treatment and prevention.

91 In this study, we explored age-related changes in the human heart. We characterized  
92 young (<30 years-old) and aged (>50-years-old) nonfailing human left ventricle (LV) samples  
93 and identified genes strongly altered with aging. We then compared the gene expression  
94 profiles of 3-month-old, 6-month-old, and 14-month-old (advanced aged) iCMs to those of  
95 human LV. Our results revealed a high degree of similarity between the advanced aged iCMs  
96 and the aged LV in terms of their stress and contractile function impairment related  
97 transcriptional signatures.

98 Next, we used chronologically aged iCMs to explore age-related changes *in vitro*. We  
99 investigated the effects of cell age on ECM therapy outcomes. Our findings showed that ECM  
100 treatment outcomes were influenced not only by cell age but also by the presence of stress  
101 conditions such as MI. Following MI-mimicking stress conditions (i.e., hypoxia), young ECM  
102 treatment led to functional recovery at all cell ages, with increased survival observed only in  
103 3-month-old iCMs.

104 In the absence of stress, the beneficial effects of young ECM treatment were limited to  
105 the younger, 3-month-old iCM group. ECM upregulated cardiac structural and functional  
106 genes, increased beating frequency and velocity, and suppressed stress-related genes and  
107 the senescence-associated secretory phenotype (SASP) in 3-month-old iCMs. Surprisingly,  
108 young ECM was pro-aging and reduced the beating of advanced aged iCMs. These results  
109 challenged the widely held assumption of the universal benefit of young ECM, raising  
110 uncertainties about the safety and efficacy of employing young ECM as a preventative  
111 treatment for CVD in the elderly.

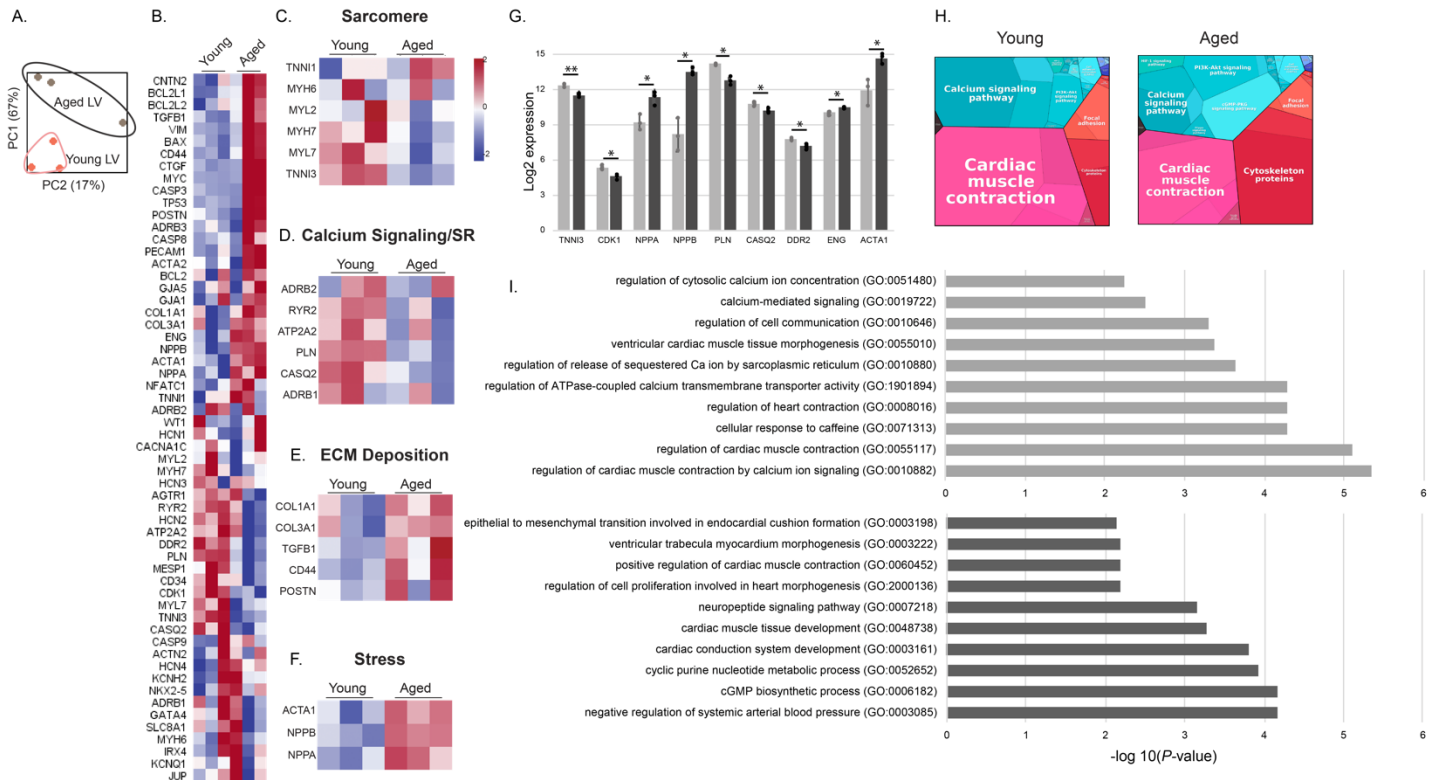
112 In conclusion, here we reported age-dependent transcriptional alterations in nonfailing  
113 human heart LVs from both young and aged subjects, and in chronologically aged iCMs. To

114 the best of our knowledge, this is the only study displaying transcriptional alterations in  
115 human LV with a focus on aging without any disease conditions. Furthermore, our results  
116 showed that chronologically aged iCMs are excellent candidates to mimic aged heart  
117 behavior and can be used to conduct CVD studies for the elderly. Using an age-appropriate  
118 cardiac model, we showed that the 'one-size-fits-all' ECM treatment approach is doomed to  
119 fail, as results are highly dependent on cell age and stress conditions.

## 120 **2. RESULTS**

### 121 **2.1. Distinct transcriptomic profiles differentiate aged human heart left ventricles** 122 **from young counterparts**

123 Left ventricles derived from healthy human hearts (young: <30-years-old, n=3 and aged: >50-  
124 years-old, n=3) were characterized. mRNA levels related to iCM maturity, function, and  
125 apoptosis were quantified and a 67% variance was detected between aged and young LV  
126 samples (**Fig. 1A-B**). Adult type sarcomeric genes (*TNNI3*, *MYH7*) and multiple Ca<sup>2+</sup> cycling/SR  
127 genes were highly expressed in young LV (**Fig. 1C-D**). Myocardial fibrillar collagens (*COL1A1*,  
128 *COL3A1*) along with other adverse cardiac remodeling contributors and stress-related genes  
129 were highly expressed in aged LV (**Fig. 1E-F**). Among screened genes, we identified 9 that  
130 were significantly altered (p<0.05) by human cardiac aging. Specifically, NPPB, a ventricular  
131 natriuretic peptide known to be secreted in the myocardium upon stress, was upregulated  
132 40-fold (p=0.017) in the aged LV (**Fig. 1G**). The KEGG pathway analysis revealed that the  
133 differentially expressed genes (DEGs) in young LV were associated with cardiac muscle  
134 contraction, calcium signaling, and focal adhesion pathways, while in aged LV they were  
135 associated with HIF-1, PI3K-Akt signaling pathways, hence cardiovascular aging, and cardiac  
136 disorders (**Fig. 1H**). The results of gene ontology (GO) analysis also showed that DEGs in  
137 young LV were significantly enriched in biological processes, including the regulation of  
138 cardiac muscle contraction by calcium ion signaling, and cell communication. Aged LV DEGs  
139 were enriched in cGMP signaling pathways, cardiac muscle tissue development, and  
140 neuropeptide signaling pathways (**Fig. 1I**). These changes in gene expression indicated that  
141 human cardiac aging mainly affected CM contractile function, Ca<sup>2+</sup> cycling, and stress  
142 response.



143 **Figure 1 Human heart left ventricle age dependent transcriptional alterations** (A) Principal  
 144 component analysis (PCA) of the gene expression data, depicting the group relationships of young  
 145 (n=3) and aged (n=3) human left ventricles (LV). The proportion of component variance is indicated as  
 146 a percentage. (B) Differential expression levels of the preselected 58 cardiac and aging specific genes  
 147 for young and aged LVs. (C–F) Heatmaps of key genes involved in distinct features of CM behavior: (C)  
 148 sarcomere, (D) calcium (Ca<sup>2+</sup>) cycling and sarcoplasmic reticulum (SR), (E) ECM deposition, and (F)  
 149 stress response. (G) Statistically altered gene expressions of young and aged human LV. Statistical  
 150 analysis was done using one-way ANOVA with post-hoc Tukey's test. \*\*p<0.01, \*p<0.05, n≥3. Data  
 151 presented as mean ± standard deviation (SD). (H) Proteomaps showing the KEGG pathways. (I) Gene  
 152 ontology analysis showing the biological processes associated with the genes overexpressed in young  
 153 and aged LVs.

## 154 2.2. Transcriptomic alterations in chronologically aged iCMs

155 Unsupervised hierarchical clustering revealed a 66% variance between young and aged iCMs  
 156 (**Fig. 2A-B**). GO analysis revealed that genes downregulated in advanced iCMs were  
 157 significantly enriched in biological processes, including DNA damage response, apoptotic  
 158 processes, and cell cycle progression. The genes that were upregulated with iCM aging were  
 159 associated with cardiac contraction, ion transport, and calcium signaling (**Supp. Fig. 1**),  
 160 indicating acquired structural and functional maturity with prolonged culture time. With  
 161 prolonged culture, the adult type sarcomeric myosins and cardiac troponin were  
 162 differentially expressed (**Fig. 2C, H**). The intermediate filament protein (*VIM*) that is highly  
 163 expressed in fetal CMs was downregulated with cellular aging. Although structurally more

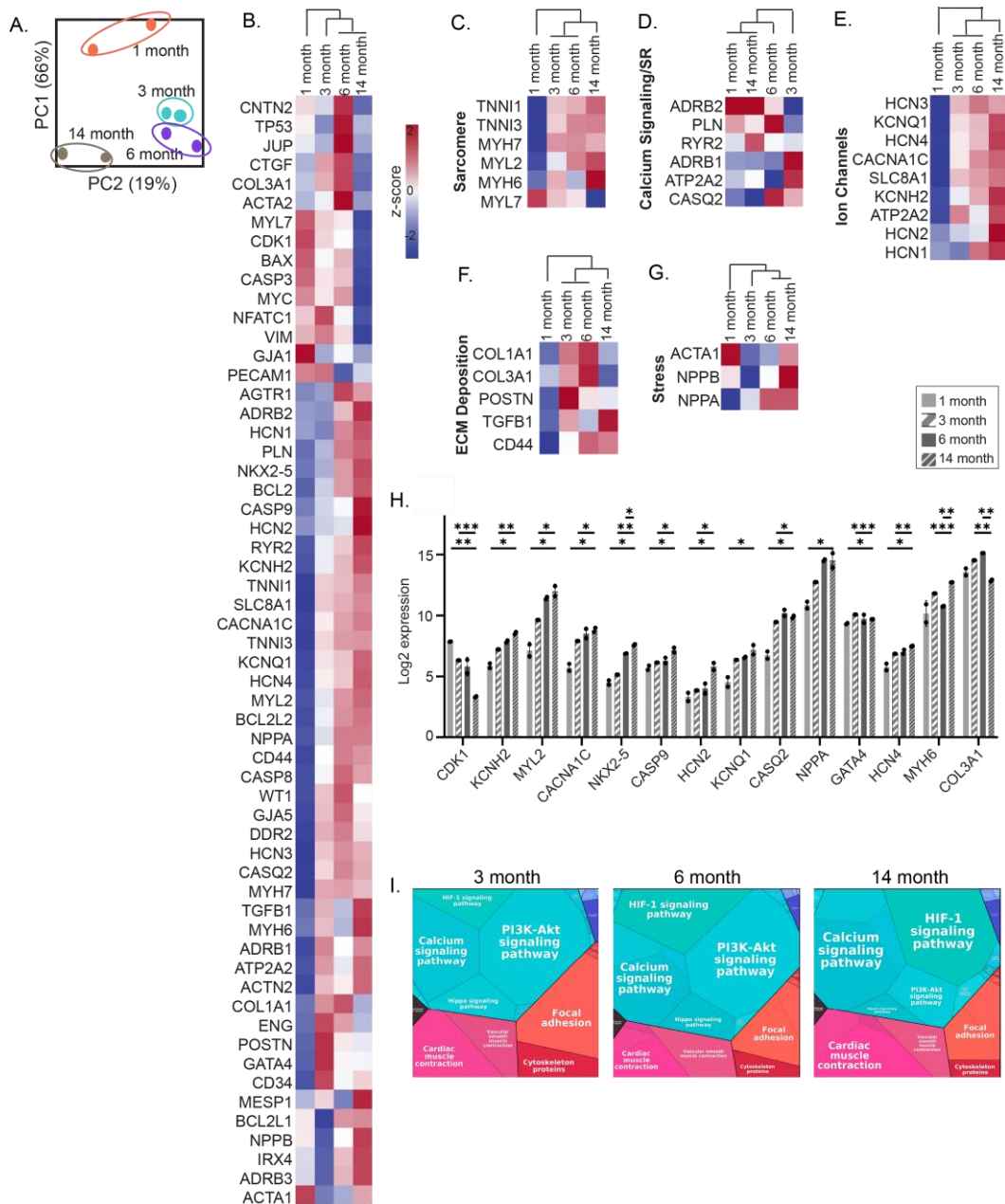
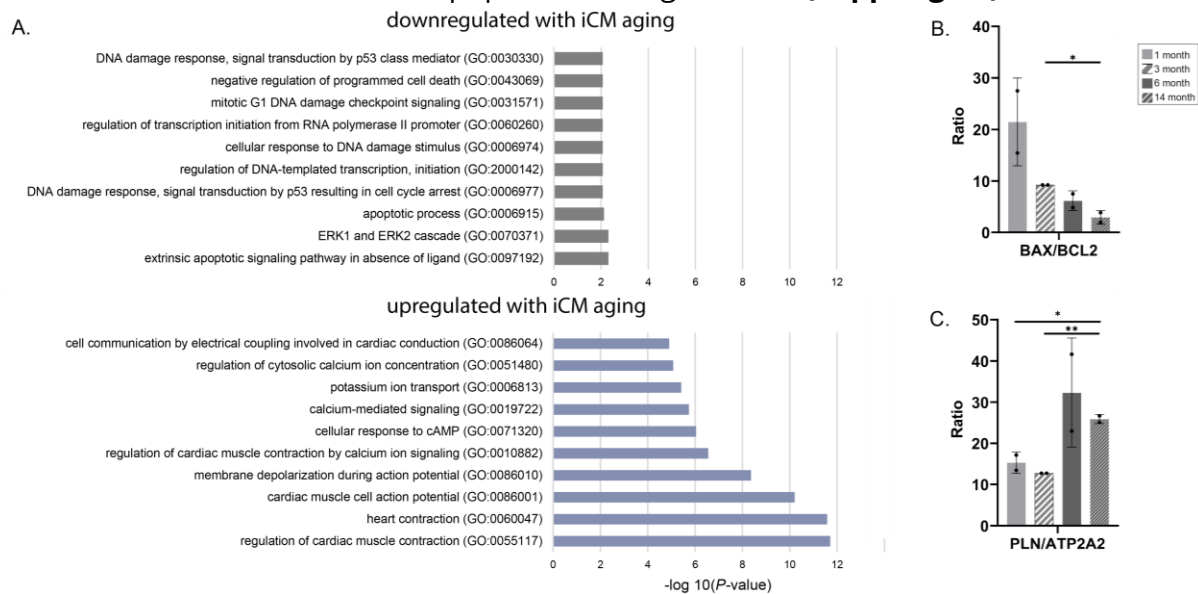


**Figure 2 iCM age-dependent transcriptional alterations** (A) Principal component analysis (PCA) of the gene expression data, depicting the group relationships of young and aged iCMs. (B) Differential expression levels of the preselected 58 cardiac and aging specific genes for iCMs. (C–G) Heatmaps of key genes involved in distinct features of CM behavior: (C) sarcomere, (D) calcium (Ca<sup>2+</sup>) cycling and sarcoplasmic reticulum (SR), (E) ion channels, (F) ECM deposition, and (G) stress response. (H) Statistically altered gene expressions of aged iCMs. Statistical analysis was done using one-way ANOVA with post-hoc Tukey's test. \*\*\* $p < 0.001$ , \*\* $p < 0.01$ , \* $p < 0.05$ ,  $n = 6$  pooled into 2 technical replicates. Data presented as mean  $\pm$  standard deviation (SD). (I) Proteomaps showing the KEGG pathways.

164 mature, advanced aged iCMs grouped together with young 1-month-old iCMs regarding their  
 165 calcium signaling and sarcomeric reticulum related expressions (**Fig. 2D**). Reduced

166 excitation-contraction coupling expressions were observed in both immature 1-month-old  
 167 and advanced aged iCMs, indicating that CMs reverted toward an impaired calcium handling  
 168 machinery as they age. The calcium handling genes that are essential for cardiac action  
 169 potential and cardiac contraction were upregulated up to 8-fold in 3- and 6-month-old iCMs,  
 170 while the negative calcium import regulator (*PLN*) was upregulated in 6- and 14-month-old  
 171 iCMs. Consequently, *PLN:ATP2A2* ratio, an indicator of reduced SERCA activity and impaired  
 172 calcium handling, was more than doubled in 6- and 14-month-old iCMs (**Supp. Fig.1C**).  
 173 Potassium and sodium channel gene expressions were gradually increased with prolonged  
 174 culture (**Fig. 2E, H**).

175 In agreement with the human LV gene profile, adverse cardiac remodeling genes that  
 176 mediate cardiac fibrosis were upregulated with iCM aging (**Fig. 2F**). As in aged LV, we  
 177 detected high levels of cardiac hypertrophy and stress related (*NPPA*, *NPPB*) expressions in  
 178 advanced aged cells. Especially *NPPA* was upregulated more than 16-fold from 1-month to  
 179 14-month of culture (**Fig. 2G**). Although experiencing more stress, and significantly  
 180 upregulated initiator caspase *CASP9* expression (**Fig. 2H**), a predictive value that determines  
 181 the susceptibility to the apoptotic signal, *BAX/BCL2* ratio revealed that advanced aged cells  
 182 were 2 times more resistant to apoptosis at the gene level (**Supp. Fig.1B**).

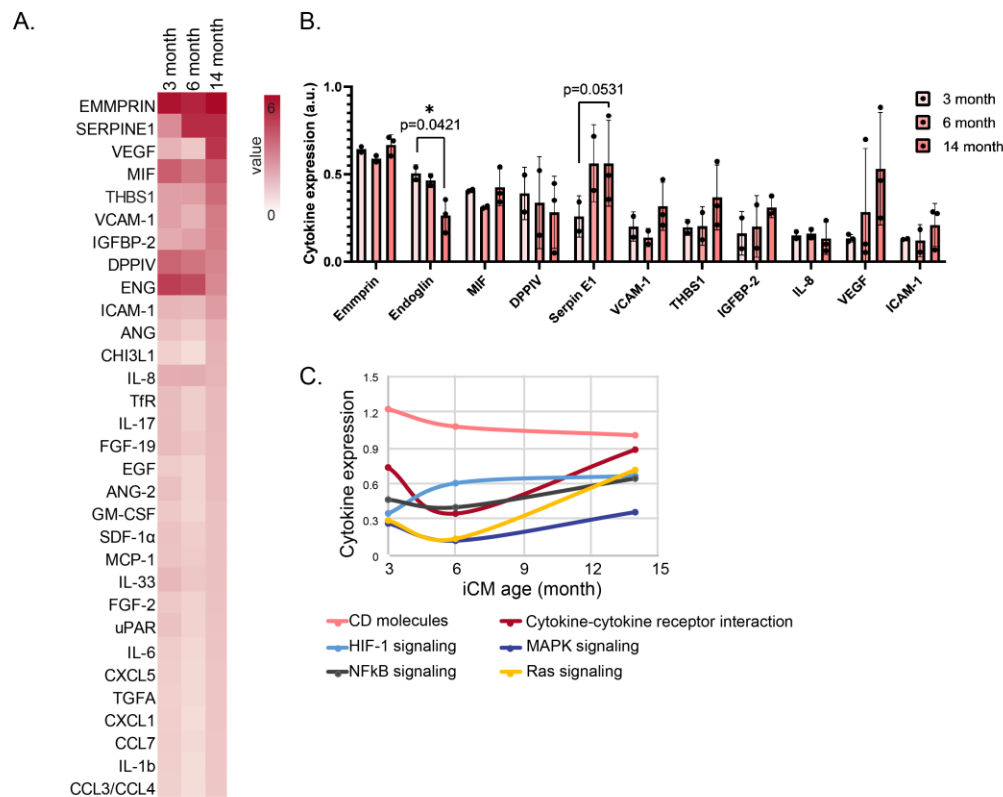


**Supplementary Figure 1. iCM age-dependent DEG alterations** (A) Gene ontology analysis showing the biological processes associated with the genes down- and up-regulated with chronological aging of iCMs. Calculated (B) *BAX/BCL2* and (C) *PLN/ATP2A2* ratios. Statistical analysis was done using one-way ANOVA with post-hoc Tukey's test. \*\*\* $p < 0.001$ , \*\* $p < 0.01$ , \* $p < 0.05$ ,  $n = 6$  pooled into 2 technical replicates. Data presented as mean  $\pm$  standard deviation (SD).

183 Additionally, cell-cycle-associated *CDK-1* gene expression was significantly downregulated  
 184 while *GATA4*, a critical regulator of cardiac regeneration, and its cofactor, *NKX2-5* expressions  
 185 were upregulated in advanced aged iCM (**Fig. 2H**). The KEGG pathway analysis of the relative  
 186 expression data further showed that regeneration mediator Hippo signaling and PI3K-Akt

187 pathways were downregulated, while HIF-1 signaling pathway and cardiac muscle  
188 contraction were upregulated in advanced aged iCMs (**Fig. 2I**).

189 Advanced aged iCMs had a larger proteome body, which might indicate increased age-  
190 associated inflammation or inflammaging. Among the highly detected proteins, the  
191 senescence mediator (SERPINE1) increased whereas the critical mediator of cardiovascular  
192 health (ENG) decreased gradually with cellular aging (**Fig. 3A-B**). In agreement with the  
193 transcriptomic alterations, the pro-aging Ras signaling pathway, master senescence  
194 associated secretory phenotype (SASP)-regulator NF-KB signaling pathway, HIF1 $\alpha$  and  
195 cytokine-cytokine receptor interaction proteins that are known to be associated with age-  
196 related degenerations in multiple organ systems[17,18] were highly expressed in advanced  
197 aged iCMs (**Fig. 3B**).



198 **Figure 3 Aged iCM cytokine expression.** (A) Heatmap showing the screened protein expressions of  
199 aged iCMs (B) Highly expressed cytokine expressions of aged iCMs. Statistical analysis was done  
200 using one-way ANOVA with post-hoc Tukey's test. \*\*\*<0.001, \*\*p<0.01, \*p<0.05, n=6 pooled into  $\geq 2$   
201 technical replicates. Data presented as mean  $\pm$  standard deviation (SD). (C) iCM age dependent  
202 changes in the cytokine expressions with respect to their role or involved pathways.  
203

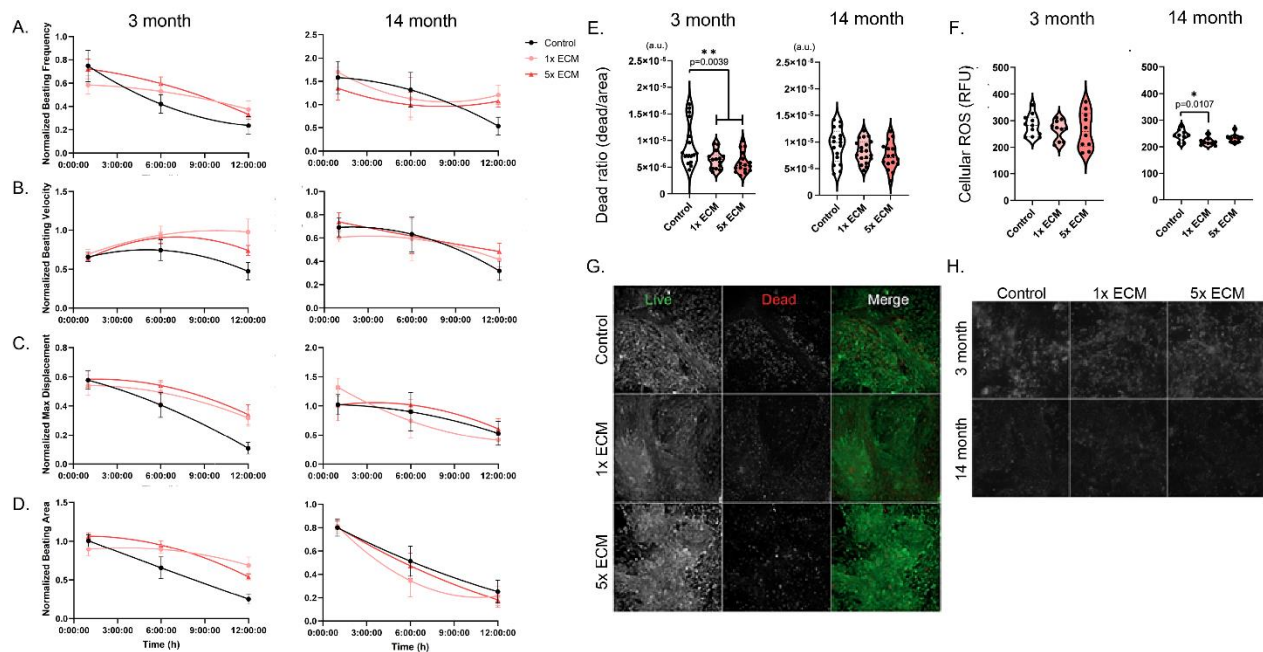
### 204 2.3. ECM treatment effect on post-MI functional recovery

205 To determine whether there were any cell age-dependent responses to the young ECM  
206 treatment for post-MI recovery, we exposed 3-month-old and advanced aged iCMs to MI-like  
207 stress conditions. The spontaneous beating of the cells was recorded before anoxia, and at



208 1h, 6h, and 12h RI to assess the beating recovery, and beating frequency (**Fig. 4A**), beating  
 209 velocity (**Fig. 4B**), maximum displacement (**Fig. 4C**), and beating area (**Fig. 4D**). 3-month-old  
 210 iCMs had higher initial beating frequencies ( $0.59\pm 0.04$  Hz) than the advanced aged iCMs  
 211 ( $0.22\pm 0.02$  Hz), hence beating values were normalized separately.

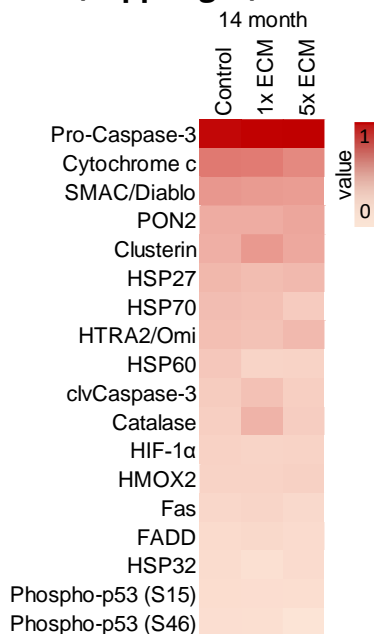
212 Within the first hour post-anoxia, 3-month-iCMs slowed down while advanced aged iCMs  
 213 displayed rapid, irregular twitches resulting in doubled beating frequencies. At the end of  
 214 12h, 1-out-of-4 samples of 3-month-old, and 4-out-of-10 samples of advanced aged iCMs  
 215 stopped beating. We observed beneficial effects of ECM treatment in both 3-month and  
 216 advanced aged iCMs. Control untreated 3-month-old group beating frequency, robustness,  
 217 and area recovered to only half of their original pre-MI values, while ECM treated groups had  
 218 faster, stronger beating across a larger area at the end of 12h normoxia (**Fig. 4A-D**). For  
 219 advanced aged iCMs, ECM treatment sustained their beating frequency (**Fig. 4A**), and the  
 220 control group frequency decreased to half of the original value. However, ECM treatment did  
 221 not affect the beating robustness or area. Regardless of the ECM, the beating area of  
 222 advanced aged iCMs was dramatically reduced.



223  
 224 **Figure 4 Post MI analysis.** Temporal changes of (A) beating frequency, (B) beating velocity of  
 225 spontaneous cell beating, (C) maximum displacement of a pixel in a frame due to spontaneous  
 226 beating, and (D) beat area (%) recorded for 12h post-MI. Left panel:3-month-old, right panel:Advanced  
 227 aged iCM. Post-MI (E) cell death ratio and (F) cellular ROS levels of 3-month-old 14-month-old  
 228 advanced aged iCMs at 12h RI. Representative images of (G) 3-month-old iCM live dead staining and  
 229 ROS generation measurement of 3-month-old and advanced aged iCM at 3h RI. Statistical analysis  
 230 was done using one-way ANOVA with post-hoc Tukey's test. \*\* $p < 0.01$ , \* $p < 0.05$ ,  $n \geq 3$ . Beating recovery  
 231 was normalized to the pre-MI initial values and data presented as mean  $\pm$  standard deviation (SD).

## 232 2.4. ECM treatment effect on the deleterious effects of MI

233 We investigated the effect of cell age on the therapeutic potential of the young ECM.  
234 Regardless of the dose used, ECM significantly lowered the dead cell count of the 3-month-  
235 old cells ( $p=0.0039$ ) while the detected cellular ROS levels were comparable (**Fig. 4E-H**). There  
236 was no survival difference in the advanced aged iCMs (**Fig. 4E**), however, mitochondrial ROS  
237 generation significantly decreased ( $p=0.0107$ ) with the ECM supplementation (**Fig. 4F**).  
238 Advanced aged cells were further screened for apoptosis-related proteins to investigate why  
239 we detected ECM effects on ROS generation but not on cell survival. When relative  
240 expressions were compared, we detected high levels of clusterin, cell protectant protein  
241 against ROS-induced apoptosis, ROS scavenger catalase, and low levels of stress proteins  
242 HSP60 and HSP70 in ECM supplemented cells. The pro-apoptotic proteins did not show a  
243 difference, yet one of the critical early mediators of apoptosis, Ser46 phosphorylation of p53  
244 level, and the apoptosis initiator, Cytochrome C gradually decreased with increasing ECM  
245 dose (**Supp. Fig. 2**).



246 **Supplementary Figure 2.** Post-MI apoptosis-related protein expression in 14-month-old advanced  
247 aged iCMs.  $n \geq 3$ .

## 250 2.5. ECM treatment effect on aged iCM expressions without any stress conditions

251 Following a 10-day treatment with young human heart LV-derived ECM at two concentrations  
252 (1x ECM: 0.1mg/ml and 5x ECM: 0.5mg/ml), we investigated the changes in transcriptome  
253 and cytokine levels. Regardless of the cell age or the ECM concentration, the treatment  
254 downregulated genes that are associated with collagen activated signaling pathways,  
255 extracellular organization, and non-cardiac cell migration, and upregulated genes associated  
256 with cardiac cell fate commitment and muscle contraction (**Fig. 5A**). GO analysis also showed  
257 that genes upregulated upon ECM treatment were enriched in regulation of glial cell  
258 differentiation, which we recently reported to be regulators of heart rate [19].

259

260 Expectedly, high concentration ECM had a greater effect on the cells, and the ECM treatment  
261 outcome depended heavily on the cell age. GO results showed that DEGs in 3-month-old  
262 iCMs were associated with functional processes such as the movement of ions and cardiac  
263 muscle contraction and relaxation. Relatedly, sarcomere, calcium signaling, and ion channel  
264 expressions were upregulated in an ECM dose dependent manner in 3-month-old iCMs (**Fig**  
265 **5B-D**). DEGs in 3-month-old and high dose ECM treated 6- and 14-month-old iCMs were  
266 involved in the positive regulation of metabolic processes in addition to cardiac contraction,  
267 and regulation of cell action potential. Adrenergic receptor (*ADRB1*) and ryanodine receptor  
268 (*RYR2*) levels which play an integral roles in excitation-contraction coupling and cardiac  
269 energy metabolism (**Fig. 5C**), increased with high concentration ECM treatment. HCN

270 channel family, Ca<sup>2+</sup> and K<sup>+</sup> channel levels in 6-month-old iCMs, and Na<sup>+</sup>/Ca<sup>2+</sup> exchanger  
 271 (*SLC8A1*) levels in advanced aged iCMs increased only when treated with high concentration  
 272 ECM. Surprisingly, DEGs in 14-month-old iCMs treated with ECM were associated with heart  
 273 development and cardiac ventricle morphogenesis (**Fig.5A**). Besides cardiac structure and  
 274 function, ECM treatment downregulated ECM deposition genes, especially in 3-month-old  
 275 iCMs. *COL3A1* was upregulated only in advanced age iCMs in an ECM dose-dependent  
 276 manner (**Fig. 5E**). Regarding cellular stress, the genes we have dominantly seen in the

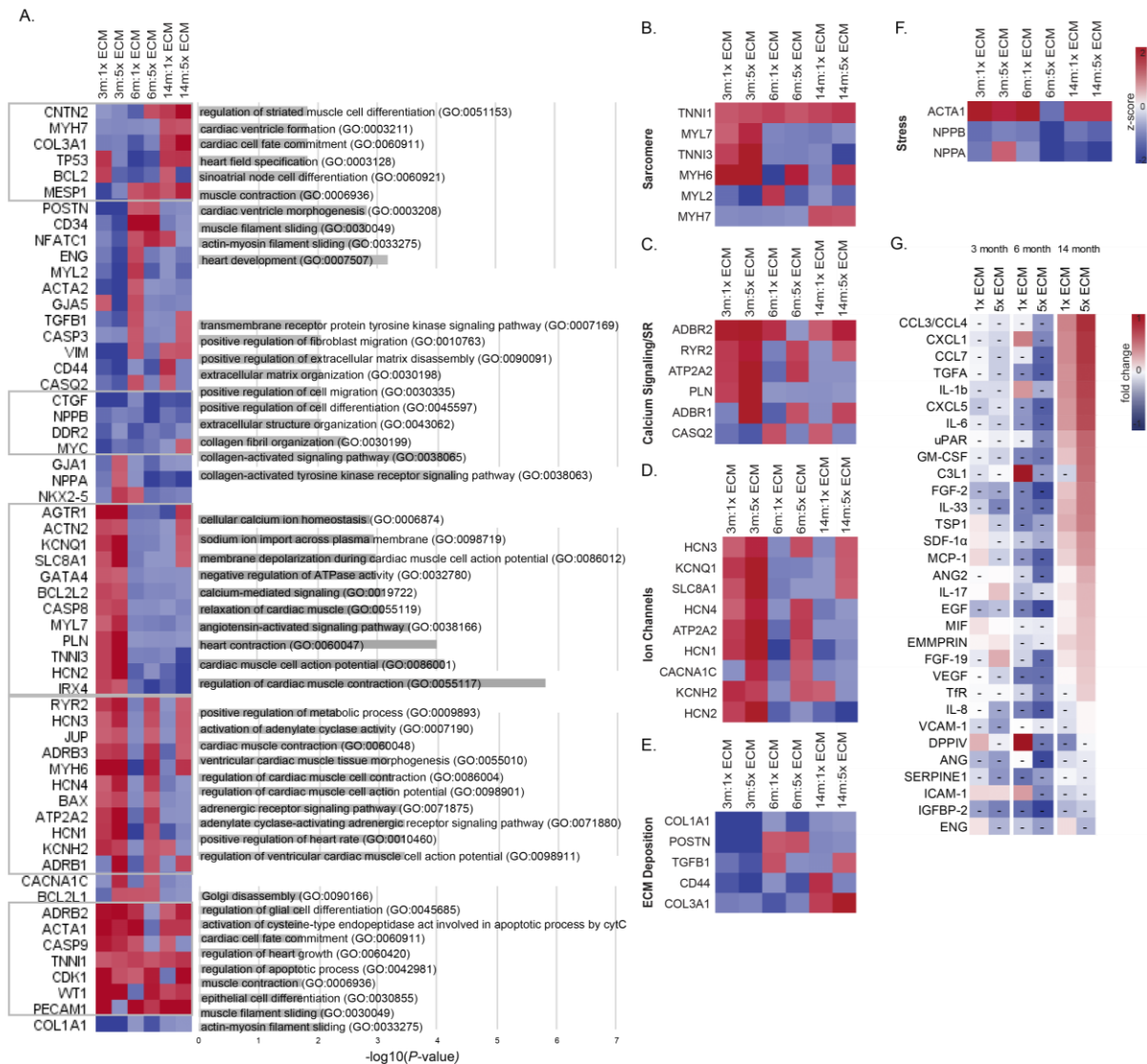


**Figure 5 ECM treatment effect on aged iCMs.** (A) Differential expression levels of the preselected 58 cardiac and aging specific genes for iCMs. Gene ontology analysis showing the biological processes associated with the up- and downregulated genes with iCM aging. (B–F) Heatmaps of key genes involved in distinct features of CM behavior: (B) sarcomere, (C) calcium (Ca<sup>2+</sup>) cycling and sarcoplasmic reticulum (SR), (D) ion channels, (E) ECM deposition, and (F) stress response. (G) Heatmap showing the screened protein expressions as a fold change from their corresponding control groups. n≥3.

277 advanced aged iCMs (*NPPA*, *NPPB*) were downregulated in all and were almost halved with  
278 the high concentration ECM treatment (**Fig. 5F**).

279 At the protein level, ECM lowered the SASP components increased with cellular aging, such  
280 as the aging markers *SERPINE1*, *IL-8*, *IGFBP-2*, and *VCAM* (**Fig. 5G**). ECM also decreased the  
281 maladaptive aging response associated cytokine, and chemokines (*THBS1*, *CHI3L1*, *IL33*) in  
282 3-month and 6-month-old iCMs. However, ECM treatment had a different effect on the  
283 advanced aged iCM than on 3-month and 6-month-old iCMs (**Fig. 5G**). Pro-aging Ras and  
284 MAPK signaling pathway proteins (i.e., *IL-1b*, *FGF2*) were highly expressed in advanced aged  
285 iCMs.

## 286 **2.6. ECM treatment effect on aged iCM beating without any stress conditions**

287 We recorded the spontaneous beating of the aged iCMs on day 3 and day 10 of the ECM  
288 treatment. The initial beating frequencies were recorded as  $0.72 \pm 0.24$  Hz for 3-month,  $0.48$   
289  $\pm 0.19$  Hz for 6-month and  $0.25 \pm 0.10$  Hz for advanced aged iCMs, expectedly decreasing with  
290 increasing cell age. ECM treatment enhanced the beating of 3-month-old iCMs, whose cells  
291 reached adult CM beating frequency ( $\sim 1$  Hz) and had significantly increased beating velocities  
292 at the end of 10-day high dose ECM treatment (**Fig. 6A-B**). However, we observed minimal if  
293 not negative effects of ECM treatment on the 6-month-old and advanced age iCM beating  
294 properties (**Fig. 6A-C**).

295 Relatedly, mitochondrial health was assessed, and we detected higher mitochondrial  
296 membrane potential (Red/Green ratio), indicating increased ATP generation potential in 3-  
297 month-old iCMs after 10-day ECM treatment (**Fig. 6D**). Interestingly, the mitochondrial  
298 potential for both 6-month and advanced aged iCMs significantly decreased after 1x ECM  
299 treatment (**Fig. 6D**). Referring to the strong correlation between mitochondrial membrane  
300 potential and ROS production, we also measured the cellular ROS levels and observed only

301 minimal changes with cell age or ECM treatment. Although ECM increased mitochondrial  
 302 activity in 3-month-old iCMs, it did not lead to increased ROS production (**Fig. 6E**).

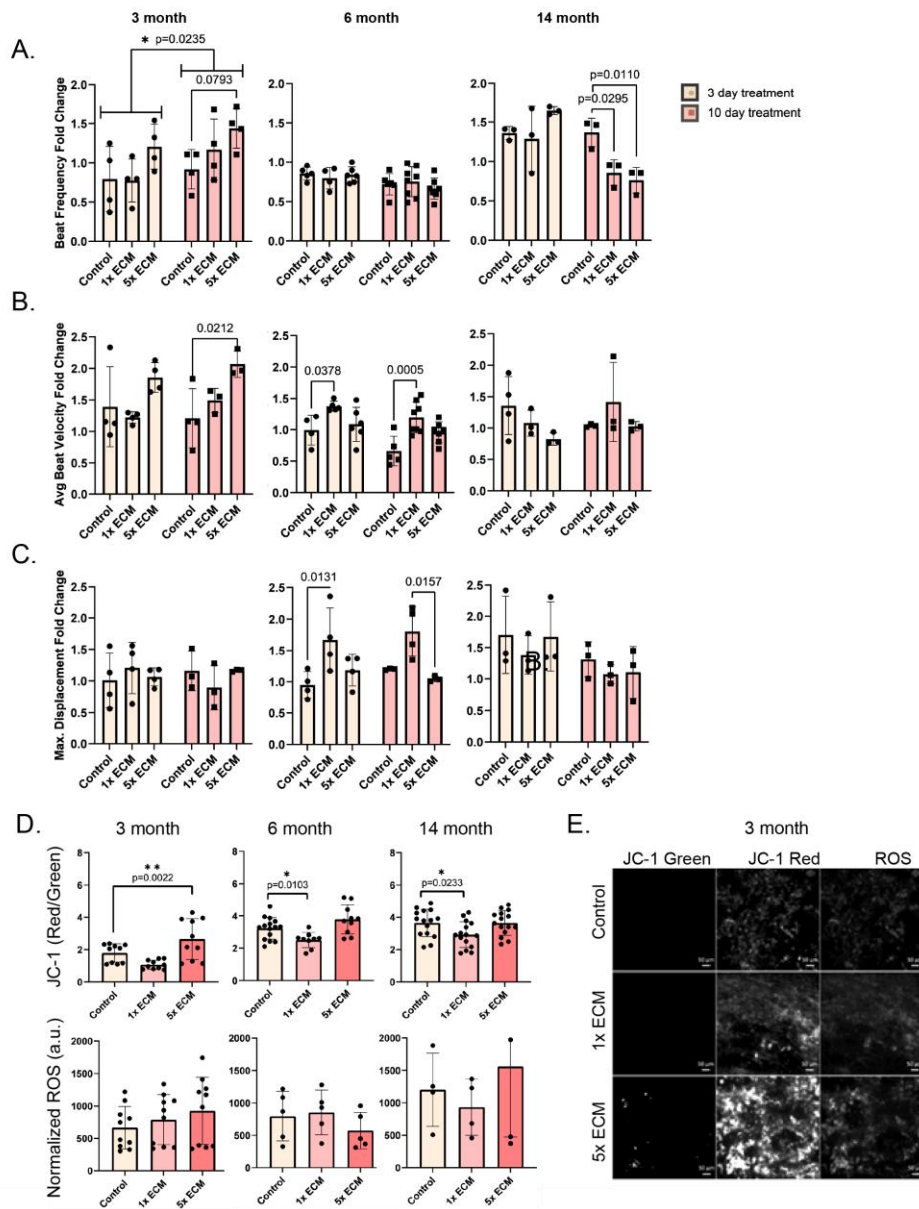


**Figure 6. ECM treatment effect on aged iCM beating kinetics.** Fold change of (A) beating frequency, (B) beating velocity of spontaneous cell beating and (C) maximum displacement of a pixel in a frame due to spontaneous beating on day 3 and 10 of treatment. (D) Quantification of mitochondrial potential (JC-1 Red/Green) as an indication of the mitochondrial health (top) and ROS levels normalized to pre-treatment measurement (bottom). Left panel: 3-month, middle-panel:6-month, right panel:advanced aged iCM. (E) 3-month-old iCM mitochondrial staining with JC-1 dye and cellular staining with ROS on the 10th day of ECM treatment. Scale bar: 50µm. Statistical analysis was done using one-way ANOVA with post-hoc Tukey's test. \*\*p<0.01, \*p<0.05, n≥3. Data presented as mean ± standard deviation (SD).

### 303 3. DISCUSSION

304 In this study, we compared aging profiles of human LV and chronologically aged iCMs, and  
305 developed aged human heart models using aged iCMs to investigate the effect of cell age on  
306 young ECM treatment outcomes. We demonstrated that young ECM is an effective treatment  
307 for MI, as it promoted the survival of cells and facilitated their beating recovery, particularly  
308 in younger iCMs. However, young ECM had unexpected negative effects as a preventative  
309 therapy for advanced aged iCMs in the absence of any stress conditions. Despite its origin in  
310 young human LV, ECM increased aging-factor expression and impaired beating of advanced  
311 aged iCMs, challenging its use for preventative purposes, especially for the elderly.

312 Many researchers have presented the human LV transcriptome in association with various  
313 diseases and conditions, yet we don't have a complete understanding of human heart aging.  
314 Age related changes reported for rodent hearts include myocyte hypertrophy, cardiac  
315 fibrosis, and reduced calcium transport across the sarcoplasmic reticulum membrane [21].  
316 Here, we have confirmed the previously described age-related pathophysiology at the  
317 transcriptomic level in human heart left ventricles (LV). We observed elevated levels of NPPA  
318 and NPPB in all aged LV samples (**Fig. 1**), which is considered a hallmark of human aging and  
319 a protective hormonal response to mechanical stress to maintain cardiovascular  
320 homeostasis [22]. Additionally, DEGs in aged LVs showed an association with cGMP and HIF-  
321 1 signaling pathways, as well as negative regulation of JUN kinase activity leading to  
322 hypertrophy and pronounced fibrosis in aged LVs [23].

323 Prolonged culture (>1-month) has typically been used as a CM maturation strategy[24–27].  
324 Therefore, little was known about the capacity of aged iCMs to mimic human cardiac aging.  
325 Here, we report for the first time that functional (i.e., beating) 14-month-old advanced aged  
326 iCMs exhibit the hallmarks of cardiac aging at both transcriptional and translational levels,  
327 including adverse cardiac modeling, hypertrophy, and SASP (**Fig. 2-3**). We observed re-  
328 expression of fetal genes (i.e., *TNNI1* and *MYH6*), induction of pre-ANF (*NPPA*), pre-BNP (*NPPB*),  
329 and *ACTA1* in the advanced aged iCMs similar to the distinct molecular phenotype associated  
330 with pressure overload-induced hypertrophy[28]. Additionally, advanced aged iCMs  
331 displayed beta-adrenergic receptor expression levels that resemble those of 1-month-old  
332 iCMs (**Fig. 2D-E**). The predominant expression of *ADRB2* (fetal-type) and low expression of  
333 *ADRB1* (adult-type) indicate  $\beta$ -adrenergic desensitization can be seen during cardiac aging as  
334 well as in immature CMs. Early studies suggest that the heart develops immature features  
335 with aging, including a dependence on transsarcolemmal calcium influx during contraction  
336 rather than calcium stored in the sarcoplasmic reticulum as in the adult heart [29,30]. Here,  
337 we showed that 14-month-old advanced aged iCMs were indeed senescent and highly similar  
338 to the aged LV at the transcriptional level.

339 We observed another phenomenon commonly seen in senescent cells. Despite high levels  
340 of initiator caspase CASP9, advanced aged iCMs had low levels of CASP3 (**Fig. 2B, H**),  
341 indicating the central apoptotic machinery downstream CASP9 was inactivated and the  
342 upregulation of CASP9 was independent of apoptosis. Additionally, the increased resistance  
343 of advanced aged iCMs to apoptosis (**Supp. Fig.1B**) suggests a survival strategy specific to

344 advanced aged iCMs, as also observed in aged olfactory bulb neurons but not in young  
345 counterparts [31]. This is known as the trade-off between senescence and apoptosis [32],  
346 and the surprising results of ECM treatment in the absence of stress conditions might be due  
347 to this delicate balance. Using the heart tissue model with different aged iCMs, we  
348 demonstrated the critical role of 'cell age' in determining ECM treatment efficacy and  
349 outcome. Consistent with previous preclinical and phase I clinical studies [6,13–16], young  
350 ECM improved post-MI beating recovery(**Fig. 4A-D**). However, the effect of ECM on the post-  
351 MI survival rate was highly cell age dependent, with only the younger cell group showing  
352 higher survival in response to ECM treatment (**Fig.4E-H**). Although young ECM enhanced  
353 oxidative stress coping mechanisms in advanced aged iCMs (**Supp. Fig. 2**), a similar effect  
354 shown in a recent study revealing the ROS scavenger activity of ECM [33], this did not  
355 translate into an increase in their survival rate. The desensitization of advanced aged cells  
356 due to reduced cellular activity and function has long been known and also observed in the  
357 human heart as it ages [6,34]. However, such a difference in previous studies has not been  
358 reported because samples are pooled together regardless of age to show the global effect  
359 of ECM therapies.

360 Current MI guidelines do not differentiate treatment based on age or sex, hence the  
361 treatment efficacies are suboptimal in the elderly and women[35]. For this study, we  
362 acknowledge the potential sex-based differences at both the gene and protein levels. A  
363 recent study on transcriptional diversity of the human heart (n=7, ages: 39-60) reported 17  
364 genes that exhibited sex-based differential expression within cardiomyocytes (i.e., *NEB*, *PBX3*)  
365 [36]. Another study on sex-related protein expressions in hypertrophic cardiomyopathy  
366 patients (n=26, ages: 48.5 ± 17.7 (F) and 49.8 ± 15.5 (M)) reported 46 proteins that were  
367 differentially expressed in the female and male groups (i.e., tubulins and HSPs)[37]. However,  
368 since we found no evidence for a sex-based differential expression in the genes or proteins  
369 of interest (**Fig. 1-3**), we didn't separate our samples by sex.

370 Studies have demonstrated the great potential of young ECM therapies in promoting post-  
371 MI recovery and regeneration, suggesting its use for preventative purposes. We  
372 demonstrated similar transcriptomic and related translational changes reported for post-MI  
373 ECM therapy results including reduced CM apoptosis, improved function, and cardiac  
374 development for 3-month-old iCMs treated with ECM (**Fig. 5A, 6**). In addition, ECM treatment  
375 improved structural and functional cardiac maturity and decreased SASP (i.e., SERPINE1,  
376 IGFBP2, and interleukins), ECM deposition, and stress-related expressions in 3-month-old  
377 iCMs in a dose dependent manner (**Fig. 5B-F**). We acknowledge the immature nature of iCMs,  
378 therefore observed maturation with the ECM treatment was expected. However, the ECM  
379 effect on SASP is noteworthy as SASP-centered approaches are emerging as alternatives to  
380 target senescence-associated diseases.

381 When we repeated the same ECM treatment for the 14-month-old advanced aged iCMs, we  
382 got unexpected results. The impact of 'cell age' on the outcome of ECM treatment was  
383 particularly significant in the absence of stress conditions. In fact, advanced aged iCMs were  
384 minimally or negatively affected by the ECM treatment. ECM increased SASP, namely CXC



385 chemokines and activated IL-6/JAK-STAT pathway (**Fig. 5G**) in advanced aged iCMs suggesting  
386 that young ECM exerted hypertrophic stress on advanced aged iCMs. As per our  
387 observations on the beating properties of advanced-aged iCMs (**Fig. 6A**), the elevation of  
388 pro-inflammatory cytokines is often associated with impaired cardiac function [38].  
389 Moreover, a highly conserved pro-aging RAS/MAPK signaling pathway was upregulated in  
390 advanced aged iCMs after ECM treatment in a dose dependent manner (**Fig. 5G**).

391 Old age is associated with worse treatment outcomes and patient age is determinant in  
392 decision-making and treatment selection in many disease conditions, including, breast  
393 cancer[39], and schizophrenia[40]. This study highlights that age is also a critical determinant  
394 in the treatment of CVDs. Despite recent advances in ECM therapies, its efficacy and  
395 outcomes in elderly patients remain limited by the lack of data. Our results clearly  
396 demonstrated that the advanced aged iCMs, representing the elderly, did not benefit equally  
397 from the post-MI young ECM treatment as the younger iCMs, and were even adversely  
398 affected in the absence of stress conditions. Therefore, age-appropriate cardiac models,  
399 such as the one presented here, are needed in the cardiac tissue engineering field to  
400 facilitate CVD therapy studies and enhance our understanding of cardiac aging.

#### 401 **4. CONCLUSION**

402 Our study revealed age-dependent transcriptional alterations in nonfailing human heart LVs,  
403 with a sole focus on aging without any co-existing disease states. Moreover, we showed that  
404 chronologically aged iCMs are excellent candidates to mimic aged heart behavior, and aged  
405 heart models using age-appropriate iCMs are valuable for studying age-dependent efficacy  
406 and outcome of the CVD therapies. Our results demonstrated that the ECM response is  
407 highly dependent on cell age and stress conditions. Therefore, there is a need for age-  
408 appropriate cardiac models in translational research to develop personalized treatments for  
409 the elderly population, and to move beyond the "one-size-fits-all" approach in ECM  
410 therapies.

#### 411 **5. MATERIALS AND METHODS**

##### 412 **5.1. Donor heart harvest**

413 De-identified human hearts that were deemed unsuitable for transplantation and donated  
414 to research, were acquired from Indiana Donor Network under the Institutional Review  
415 Board (IRB) approval for deceased donor tissue recovery. Human heart tissues were grouped  
416 as young (from <30 years-old patients, n=3), and aged (from 50< years-old patients, n=3). For  
417 storage, hearts were dissected into its chambers and kept separately in a -80°C freezer until  
418 use. We only used the young left ventricles (n=3) for the ECM treatments

##### 419 **5.2. Decellularization of human heart tissue for matrix preparation**

420 Left ventricles from young donors were sectioned and decellularized following previous  
421 decellularization protocol [41]. Briefly, we first stripped the fatty tissue around the left  
422 ventricular myocardial tissue and sliced the tissues in thin sections (<1mm). To decellularize,  
423 tissues were washed in 1% (wt/vol) sodium dodecyl sulfate (SDS) (VWR, #97062) for 24 hours  
424 or until white transparent tissue was obtained, then in 1% (wt/vol) Triton 100-X (Sigma-

425 Aldrich, #A16046) for 30 minutes. After decellularization, samples were washed thoroughly  
426 with DI water to remove any residual detergent. To delipidize, tissues were washed with the  
427 isopropanol (IPA) for 3 hours then rehydrated in DI and treated with 50U/ml DNase (Millipore  
428 Sigma, #10104159001) for 8 hours followed by an overnight DI rinse. All steps were  
429 conducted with constant agitation at RT.

430 Prepared ECMs were lyophilized and pulverized with liquid nitrogen. ECM powder was  
431 digested in a 1 mg/mL pepsin (Sigma-Aldrich, #P6887) in 0.1M HCl (10:1, w/w, dry  
432 ECM:pepsin) at RT with constant stirring until a homogeneous solution was obtained. The  
433 insoluble remnants were removed by centrifugation, the supernatant was neutralized using  
434 1M NaOH solution, and used immediately to prevent degradation. Prior to experiments, we  
435 measured the total protein concentrations using Rapid Gold BCA Assay (Thermo Scientific, #  
436 A53227) and diluted ECM solutions to either 0.01 mg/ml (1x) or 0.05 mg/ml (5x) with the  
437 culture media.

### 438 **5.3. Human iPSC cell line**

439 The cell line used in this study is DiPS 1016 SeVA (RRID: CVCL\_UK18) from human dermal  
440 fibroblasts obtained from Harvard Stem Cell Institute iPS Core Facility. Cells were cultured in  
441 humidified incubators at 37 °C and 5% CO<sub>2</sub>. Human iPS cells were cultured routinely in  
442 mTeSR-1 media (StemCell Technologies, #05825) on 1% Geltrex-coated plates (Invitrogen,  
443 #A1413201). At 80-85% confluency, cells were passaged using Accutase (StemCell  
444 Technologies, #07920) and seeded at  $1.5 \times 10^5$  cells/cm<sup>2</sup> on well plates with Y-27632 (ROCK  
445 inhibitor, 5 μM), (StemCell Technologies, #129830-38-2) in mTeSR-1 media. The culture was  
446 maintained with daily media changes until 90% confluency was reached.

### 447 **5.4. Culturing iPSC-derived cardiomyocytes**

448 Once 90% confluency was reached, cardiac differentiation was initiated following canonical  
449 Wnt pathway [42]. To direct cardiac differentiation, cells are sequentially treated with  
450 CHIR99021 (12 μM) (Stemcell Technologies, #72052) for 24 hours followed by RPMI 1640  
451 medium with B-27 supplement without insulin (2%) (Gibco, #A1895601) (CM(-)). Cells were  
452 then treated with Wnt pathway inhibitor IWP-4 (5 μM) (Stemcell Technologies, #72552) for 48  
453 hours followed by CM(-) for 48 hours. From day 9 on, cells were maintained in RPMI 1640  
454 medium with B-27 (2%) (Gibco, #17504044) (CM(+)) and media was changed every 3 days.  
455 iCMs were cultured for 3-months, 5-6-months and 13-14-months.

### 456 **5.5. ECM treatment experiments**

457 Myocardial infarction (MI) experiment was mimicked in two parts as ischemic phase (I) and  
458 reperfusion injury (RI). Aged cells were incubated under anoxic conditions (37 °C, 5% CO<sub>2</sub>,  
459 0.1% O<sub>2</sub>) for 3 hours (I), then moved to normoxic conditions (21% O<sub>2</sub>) for 12 hours (RI). During  
460 ischemia, cells were incubated in anoxia-equilibrated RPMI 1640 medium without glucose  
461 (Corning, #10043CV) with B-27 supplement without antioxidants (2%) (Gibco, #10889038).  
462 During RI, cells were incubated with CM(+) medium alone or supplemented with  
463 decellularized ECM (1x or 5x concentration). For functional recovery, spontaneous beatings  
464 were recorded at 1h, 3h, 6h and 12h RI. At 3h RI, cellular ROS was measured and at 12h RI

465 apoptosis-related proteome was profiled (R&D Systems, #ARY009), and survival rate was  
466 measured via live/dead staining (Abcam, #ab115347).

467 Aged cells were treated with decellularized ECM for 10 days and control groups were  
468 maintained in CM(+) media throughout the experiment. Cells were screened for their relative  
469 cytokine content and gene expressions before and after ECM treatment. After treatment,  
470 spontaneous beating of the cells as well as mitochondrial health (ThermoFisher, MitoProbe  
471 JC-1, #M34152) and cellular ROS (Abcam, Cellular ROS Assay #ab186029) were assessed.

#### 472 **5.6. RNA Isolation**

473 Cells were rinsed with PBS, collected with trypsin, and stored in a -80°C freezer for future  
474 RNA isolation. For RNA isolation, frozen cells were thawed and centrifuged to remove the  
475 freezing media. The pellet was then processed following the RNeasy Mini Kit (Qiagen,  
476 #74104) protocol. Briefly, cells were disrupted using the lysis buffer and same volume  
477 ethanol added to the lysate. The sample is then applied to the RNeasy mini spin column,  
478 collected on the membrane, and finally RNA was eluted in RNase-free water. RNA purity was  
479 confirmed, concentration was measured using a Nanodrop 2000 spectrophotometer, and  
480 samples were sent to the core facility at Ohio State University.

#### 481 **5.7. Gene Expression Analysis**

482 mRNA levels were quantified using NanoString Technology. An nCounter custom codeset  
483 was designed for the identification of genes of interest related to iCM maturity, function and  
484 apoptosis with a total of 64 genes including 5 housekeeping genes  
485 (*B2M*, *EEF1A1*, *GAPDH*, *RNPS1*, and *SRP14*), selected based on a publication [43]. RNA inputs of  
486 100 ng were used for hybridization and placed on a cartridge for the NanoString reader. The  
487 output files (RCC files) were loaded into nSolver Analysis software. Data was run for quality  
488 control and background normalization, then genes of interest were normalized to the  
489 housekeeping genes. For visualization purposes, heatmap of  $\log_2FC$  for the differentially  
490 expressed genes was generated using the nSolver analysis software v4.0. Complete linkage  
491 hierarchical clustering method with Euclidean distance was used to cluster the human  
492 tissues and iCMs.

493 Gene Ontology (GO) Analysis was performed on the obtained relative expression data.  
494 Comprehensive analysis was performed using an online database via EnrichR for biological  
495 processes and enrichment analysis[44]. Data was extracted from the output dataset and  
496 graphed manually using the p-value provided. Proteomic interactions of the same relative  
497 expression data were also classified through KEGG-based proteomapping software[45] and  
498 are presented as obtained.

#### 499 **5.8. Proteome Analysis**

500 The relative cytokine content of the aged iCMs before and after ECM treatment and of the  
501 decellularized human heart ECM were obtained using the Human XL Cytokine Array Kit  
502 (ARY022B, R&D Systems). Briefly, cell lysates were obtained by disrupting the cells using the  
503 lysis buffer supplemented with protease inhibitor cocktail and tissue extracts were obtained  
504 by 1% Triton-X incubation. The relative expression levels of apoptosis related proteins of post

505 I/RI iCMs (n=3) were analyzed using the Proteome Profiler Human Apoptosis Array (R&D  
506 Systems, #ARY009), according to the manufacturer's instructions.  
507 For all, protein concentrations were normalized before starting the arrays and incubated  
508 overnight with pre-blocked membranes at 4°C. At the end, the unbound proteins were rinsed  
509 away, the membranes were incubated with the Streptavidin-HRP, then developed using  
510 chemiluminescent detection reagent mixture. For quantification, the background was  
511 removed, and the pixel density of each spot was measured using ImageJ.

### 512 **5.9. Beating Analysis**

513 A block-matching algorithm was performed using MATLAB as described previously[6].  
514 Briefly, spontaneous beating of iCMs were recorded (n=3-4 ROI per sample) and the beating  
515 frequency, average beating velocity, average maximum displacement, and beat area (%)  
516 were calculated. To analyze, measurements were normalized to pre-treatment values.

### 517 **5.10. Statistical Analysis**

518 The mean  $\pm$  standard deviation (SD) was reported for all replicates. One-way ANOVA with  
519 post-hoc Tukey's test was used to assess the statistically significant differences using  
520 GraphPad Prism version 8. All  $p$  values reported were two-tailed, and  $p < 0.05$  was considered  
521 statistically significant. Sample size (n)  $\geq 3$  for individual experiments.

### 522 **Acknowledgements**

523 This work was supported by the National Science Foundation CBET grant number [1651385]  
524 and [NSF-1805157]. We would also like to thank Dr. Keith L March and Indiana Donor  
525 Network for facilitating the human tissue acquisition and Dr. Bradley Ellis for transportation.  
526

### 527 **Data availability statement**

528 The raw/processed data required to reproduce these findings can be shared upon  
529 reasonable request.

### 530 **Ethics Statement**

531 Deidentified human hearts from donors that were deemed unsuitable for transplantation  
532 and donated to research were collected through the Indiana Donor Network under the  
533 Institutional Review Board (IRB) approval for deceased donor tissue recovery. All human  
534 tissue collection conformed to the Declaration of Helsinki.

### 535 **References**

536 [1] S.S. Virani, A. Alonso, E.J. Benjamin, M.S. Bittencourt, C.W. Callaway, A.P. Carson, A.M.  
537 Chamberlain, A.R. Chang, S. Cheng, F.N. Delling, L. Djousse, M.S.V. Elkind, J.F. Ferguson,  
538 M. Fornage, S.S. Khan, B.M. Kissela, K.L. Knutson, T.W. Kwan, D.T. Lackland, T.T. Lewis,  
539 J.H. Lichtman, C.T. Longenecker, M.S. Loop, P.L. Lutsey, S.S. Martin, K. Matsushita, A.E.  
540 Moran, M.E. Mussolino, A.M. Perak, W.D. Rosamond, G.A. Roth, U.K.A. Sampson, G.M.  
541 Satou, E.B. Schroeder, S.H. Shah, C.M. Shay, N.L. Spartano, A. Stokes, D.L. Tirschwell, L.B.  
542 VanWagner, C.W. Tsao, On behalf of the American Heart Association Council on  
543 Epidemiology and Prevention Statistics Committee and Stroke Statistics Subcommittee,

- 544 Heart Disease and Stroke Statistics—2020 Update: A Report From the American Heart  
545 Association, *Circulation*. 141 (2020). <https://doi.org/10.1161/CIR.0000000000000757>.
- 546 [2] A. Kochar, A.Y. Chen, P.P. Sharma, N.J. Pagidipati, G.C. Fonarow, P.A. Cowper, M.T. Roe,  
547 E.D. Peterson, T.Y. Wang, Long-Term Mortality of Older Patients With Acute Myocardial  
548 Infarction Treated in US Clinical Practice, *J. Am. Heart Assoc. Cardiovasc. Cerebrovasc.*  
549 *Dis.* 7 (2018). <https://doi.org/10.1161/JAHA.117.007230>.
- 550 [3] D. Berliner, J. Bauersachs, Drug treatment of heart failure in the elderly, *Herz*. 43 (2018)  
551 207–213. <https://doi.org/10.1007/s00059-017-4668-9>.
- 552 [4] C. Stamm, B. Nasser, T. Drews, R. Hetzer, Cardiac cell therapy: A realistic concept for  
553 elderly patients?, *Exp. Gerontol.* 43 (2008) 679–690.  
554 <https://doi.org/10.1016/j.exger.2008.05.008>.
- 555 [5] A. Sheydina, D.R. Riordon, K.R. Boheler, Molecular mechanisms of cardiomyocyte aging,  
556 *Clin. Sci. Lond. Engl.* 1979. 121 (2011) 315–329. <https://doi.org/10.1042/CS20110115>.
- 557 [6] S.G. Ozcebe, G. Bahcecioglu, X.S. Yue, P. Zorlutuna, Effect of cellular and ECM aging on  
558 human iPSC-derived cardiomyocyte performance, maturity and senescence,  
559 *Biomaterials*. 268 (2021) 120554. <https://doi.org/10.1016/j.biomaterials.2020.120554>.
- 560 [7] Y.S. Kim, M. Majid, A.J. Melchiorri, A.G. Mikos, Applications of decellularized extracellular  
561 matrix in bone and cartilage tissue engineering, *Bioeng. Transl. Med.* 4 (2018) 83–95.  
562 <https://doi.org/10.1002/btm2.10110>.
- 563 [8] T. Ren, A. Faust, Y. van der Merwe, B. Xiao, S. Johnson, A. Kandakatla, V.S. Gorantla, S.F.  
564 Badylak, K.M. Washington, M.B. Steketee, Fetal extracellular matrix nerve wraps locally  
565 improve peripheral nerve remodeling after complete transection and direct repair in  
566 rat, *Sci. Rep.* 8 (2018) 4474. <https://doi.org/10.1038/s41598-018-22628-8>.
- 567 [9] H. Shimoda, H. Yagi, H. Higashi, K. Tajima, K. Kuroda, Y. Abe, M. Kitago, M. Shinoda, Y.  
568 Kitagawa, Decellularized liver scaffolds promote liver regeneration after partial  
569 hepatectomy, *Sci. Rep.* 9 (2019) 12543. <https://doi.org/10.1038/s41598-019-48948-x>.
- 570 [10] D. Bejleri, M.E. Davis, Decellularized Extracellular Matrix Materials for Cardiac Repair  
571 and Regeneration, *Adv. Healthc. Mater.* 8 (2019) 1801217.  
572 <https://doi.org/10.1002/adhm.201801217>.
- 573 [11] E. Maghin, P. Garbati, R. Quarto, M. Piccoli, S. Bollini, Young at Heart: Combining  
574 Strategies to Rejuvenate Endogenous Mechanisms of Cardiac Repair, *Front. Bioeng.*  
575 *Biotechnol.* 8 (2020). <https://www.frontiersin.org/article/10.3389/fbioe.2020.00447>.
- 576 [12] C. Williams, K.P. Quinn, I. Georgakoudi, L.D. Black, Young developmental age cardiac  
577 extracellular matrix promotes the expansion of neonatal cardiomyocytes in vitro, *Acta*  
578 *Biomater.* 10 (2014). <https://doi.org/10.1016/j.actbio.2013.08.037>.
- 579 [13] J.M. Singelyn, P. Sundaramurthy, T.D. Johnson, P.J. Schup-Magoffin, D.P. Hu, D.M. Faulk,  
580 J. Wang, K.M. Mayle, K. Bartels, M. Salvatore, A.M. Kinsey, A.N. DeMaria, N. Dib, K.L.  
581 Christman, Catheter-Deliverable Hydrogel Derived From Decellularized Ventricular  
582 Extracellular Matrix Increases Endogenous Cardiomyocytes and Preserves Cardiac  
583 Function Post-Myocardial Infarction, *J. Am. Coll. Cardiol.* 59 (2012) 751–763.  
584 <https://doi.org/10.1016/j.jacc.2011.10.888>.
- 585 [14] Z. Wang, D.W. Long, Y. Huang, W.C. Chen, K. Kim, Y. Wang, Decellularized Neonatal  
586 Cardiac Extracellular Matrix Prevents Widespread Ventricular Remodeling in Adult

- 587 Mammals after Myocardial Infarction, *Acta Biomater.* 87 (2019) 140–151.  
588 <https://doi.org/10.1016/j.actbio.2019.01.062>.
- 589 [15] W.C.W. Chen, Z. Wang, M.A. Missinato, D.W. Park, D.W. Long, H.-J. Liu, X. Zeng, N.A. Yates,  
590 K. Kim, Y. Wang, Decellularized zebrafish cardiac extracellular matrix induces  
591 mammalian heart regeneration, *Sci. Adv.* 2 (2016) e1600844.  
592 <https://doi.org/10.1126/sciadv.1600844>.
- 593 [16] J.H. Traverse, T.D. Henry, N. Dib, A.N. Patel, C. Pepine, G.L. Schaer, J.A. DeQuach, A.M.  
594 Kinsey, P. Chamberlin, K.L. Christman, First-in-Man Study of a Cardiac Extracellular  
595 Matrix Hydrogel in Early and Late Myocardial Infarction Patients, *JACC Basic Transl. Sci.*  
596 4 (2019) 659–669. <https://doi.org/10.1016/j.jacbts.2019.07.012>.
- 597 [17] V.M. Shahrokhi, A. Ravari, T. Mirzaei, M. Zare-Bidaki, G. Asadikaram, M.K. Arababadi, IL-  
598 17A and IL-23: plausible risk factors to induce age-associated inflammation in  
599 Alzheimer’s disease, *Immunol. Invest.* 47 (2018) 812–822.  
600 <https://doi.org/10.1080/08820139.2018.1504300>.
- 601 [18] I.M. Rea, D.S. Gibson, V. McGilligan, S.E. McNerlan, H.D. Alexander, O.A. Ross, Age and  
602 Age-Related Diseases: Role of Inflammation Triggers and Cytokines, *Front. Immunol.* 9  
603 (2018). <https://doi.org/10.3389/fimmu.2018.00586>.
- 604 [19] N.L. Kikel-Coury, J.P. Brandt, I.A. Correia, M.R. O’Dea, D.F. DeSantis, F. Sterling, K.  
605 Vaughan, G. Ozcebe, P. Zorlutuna, C.J. Smith, Identification of astroglia-like cardiac  
606 nexus glia that are critical regulators of cardiac development and function, *PLOS Biol.*  
607 19 (2021) e3001444. <https://doi.org/10.1371/journal.pbio.3001444>.
- 608 [20] M.J. Broun, R. Wambolt, H. Cen, P. Asghari, R.F. Albu, J. Han, D. McAfee, M. Pourrier,  
609 N.E. Scott, L. Bohunek, J.E. Kulpa, S.R.W. Chen, D. Fedida, R.W. Brownsey, C.H. Borchers,  
610 L.J. Foster, T. Mayor, E.D.W. Moore, M.F. Allard, J.D. Johnson, Cardiac Ryanodine  
611 Receptor (Ryr2)-mediated Calcium Signals Specifically Promote Glucose Oxidation via  
612 Pyruvate Dehydrogenase, *J. Biol. Chem.* 291 (2016) 23490–23505.  
613 <https://doi.org/10.1074/jbc.M116.756973>.
- 614 [21] S.-K. Park, T.A. Prolla, Lessons learned from gene expression profile studies of aging and  
615 caloric restriction, *Ageing Res. Rev.* 4 (2005) 55–65.  
616 <https://doi.org/10.1016/j.arr.2004.09.003>.
- 617 [22] J.C. Burnett, X. Ma, P.M. McKie, Myocardial Aging, the Cardiac Atria, and BNP, *J. Am. Coll.*  
618 *Cardiol.* 74 (2019) 1801–1803. <https://doi.org/10.1016/j.jacc.2019.08.020>.
- 619 [23] R. Windak, J. Müller, A. Felley, A. Akhmedov, E.F. Wagner, T. Pedrazzini, G. Sumara, R.  
620 Ricci, The AP-1 Transcription Factor c-Jun Prevents Stress-Imposed Maladaptive  
621 Remodeling of the Heart, *PLOS ONE.* 8 (2013) e73294.  
622 <https://doi.org/10.1371/journal.pone.0073294>.
- 623 [24] S. Vučković, R. Dinani, E.E. Nollet, D.W.D. Kuster, J.W. Buikema, R.H. Houtkooper, M.  
624 Nabben, J. van der Velden, B. Goversen, Characterization of cardiac metabolism in iPSC-  
625 derived cardiomyocytes: lessons from maturation and disease modeling, *Stem Cell Res.*  
626 *Ther.* 13 (2022) 332. <https://doi.org/10.1186/s13287-022-03021-9>.
- 627 [25] T. Kamakura, T. Makiyama, K. Sasaki, Y. Yoshida, Y. Wuriyanghai, J. Chen, T. Hattori, S.  
628 Ohno, T. Kita, M. Horie, S. Yamanaka, T. Kimura, Ultrastructural Maturation of Human-

- 629 Induced Pluripotent Stem Cell-Derived Cardiomyocytes in a Long-Term Culture, *Circ. J.*  
630 77 (2013) 1307–1314. <https://doi.org/10.1253/circj.CJ-12-0987>.
- 631 [26] A. Hasan, N. Mohammadi, A. Nawaz, T. Kodagoda, I. Diakonov, S.E. Harding, J. Gorelik,  
632 Age-Dependent Maturation of iPSC-CMs Leads to the Enhanced Compartmentation of  
633  $\beta$ 2AR-cAMP Signalling, *Cells*. 9 (2020) 2275. <https://doi.org/10.3390/cells9102275>.
- 634 [27] J. Lewandowski, N. Rozwadowska, T.J. Kolanowski, A. Malcher, A. Zimna, A. Rugowska, K.  
635 Fiedorowicz, W. Łabędź, Ł. Kubaszewski, K. Chojnacka, K. Bednarek-Rajewska, P.  
636 Majewski, M. Kurpisz, The impact of in vitro cell culture duration on the maturation of  
637 human cardiomyocytes derived from induced pluripotent stem cells of myogenic origin,  
638 *Cell Transplant*. 27 (2018) 1047–1067. <https://doi.org/10.1177/0963689718779346>.
- 639 [28] A. Calderone, N. Takahashi, N.J. Izzo Jr, C.M. Thaik, W.S. Colucci, Pressure- and Volume-  
640 Induced Left Ventricular Hypertrophies Are Associated With Distinct Myocyte  
641 Phenotypes and Differential Induction of Peptide Growth Factor mRNAs, *Circulation*. 92  
642 (1995) 2385–2390. <https://doi.org/10.1161/01.CIR.92.9.2385>.
- 643 [29] R.A. Bassani, Transient outward potassium current and Ca<sup>2+</sup> homeostasis in the heart:  
644 beyond the action potential, *Braz. J. Med. Biol. Res.* 39 (2006) 393–403.  
645 <https://doi.org/10.1590/S0100-879X2006000300010>.
- 646 [30] D.R. Sawmiller, R.A. Fenton, J.G. Dobson, Myocardial adenosine A1-receptor sensitivity  
647 during juvenile and adult stages of maturation, *Am. J. Physiol.-Heart Circ. Physiol.* 274  
648 (1998) H627–H635. <https://doi.org/10.1152/ajpheart.1998.274.2.H627>.
- 649 [31] S. Ohsawa, S. Hamada, H. Asou, K. Kuida, Y. Uchiyama, H. Yoshida, M. Miura, Caspase-9  
650 activation revealed by semaphorin 7A cleavage is independent of apoptosis in the aged  
651 olfactory bulb, *J. Neurosci. Off. J. Soc. Neurosci.* 29 (2009) 11385–11392.  
652 <https://doi.org/10.1523/JNEUROSCI.4780-08.2009>.
- 653 [32] L. Hu, H. Li, M. Zi, W. Li, J. Liu, Y. Yang, D. Zhou, Q.-P. Kong, Y. Zhang, Y. He, Why Senescent  
654 Cells Are Resistant to Apoptosis: An Insight for Senolytic Development, *Front. Cell Dev.*  
655 *Biol.* 10 (2022) 822816. <https://doi.org/10.3389/fcell.2022.822816>.
- 656 [33] R.M. Wang, J.M. Mesfin, J. Hunter, P. Cattaneo, N. Guimarães-Camboa, R.L. Braden, C.  
657 Luo, R.C. Hill, M. Dzieciatkowska, K.C. Hansen, S. Evans, K.L. Christman, Myocardial  
658 matrix hydrogel acts as a reactive oxygen species scavenger and supports a proliferative  
659 microenvironment for cardiomyocytes, *Acta Biomater.* 152 (2022) 47–59.  
660 <https://doi.org/10.1016/j.actbio.2022.08.050>.
- 661 [34] S.C. Park, Survive or thrive: tradeoff strategy for cellular senescence, *Exp. Mol. Med.* 49  
662 (2017) e342–e342. <https://doi.org/10.1038/emm.2017.94>.
- 663 [35] B. Ibanez, S. James, S. Agewall, M.J. Antunes, C. Bucciarelli-Ducci, H. Bueno, A.L.P.  
664 Caforio, F. Crea, J.A. Goudevenos, S. Halvorsen, G. Hindricks, A. Kastrati, M.J. Lenzen, E.  
665 Prescott, M. Roffi, M. Valgimigli, C. Varenhorst, P. Vranckx, P. Widimský, ESC Scientific  
666 Document Group, 2017 ESC Guidelines for the management of acute myocardial  
667 infarction in patients presenting with ST-segment elevation: The Task Force for the  
668 management of acute myocardial infarction in patients presenting with ST-segment  
669 elevation of the European Society of Cardiology (ESC), *Eur. Heart J.* 39 (2018) 119–177.  
670 <https://doi.org/10.1093/eurheartj/ehx393>.

- 671 [36] N.R. Tucker, M. Chaffin, S.J. Fleming, A.W. Hall, V.A. Parsons, K.C. Bedi, A.-D. Akkad, C.N.  
672 Herndon, A. Arduini, I. Papangelis, C. Roselli, F. Aguet, S.H. Choi, K.G. Ardlie, M. Babadi,  
673 K.B. Margulies, C.M. Stegmann, P.T. Ellinor, Transcriptional and Cellular Diversity of the  
674 Human Heart, *Circulation*. 142 (2020) 466–482.  
675 <https://doi.org/10.1161/CIRCULATIONAHA.119.045401>.
- 676 [37] M. Schuldt, L.M. Dorsch, J.C. Knol, T.V. Pham, T. Schelfhorst, S.R. Piersma, C. dos  
677 Remedios, M. Michels, C.R. Jimenez, D.W.D. Kuster, J. van der Velden, Sex-Related  
678 Differences in Protein Expression in Sarcomere Mutation-Positive Hypertrophic  
679 Cardiomyopathy, *Front. Cardiovasc. Med.* 8 (2021) 612215.  
680 <https://doi.org/10.3389/fcvm.2021.612215>.
- 681 [38] H. Jin, T. Fujita, M. Jin, R. Kurotani, Y. Hidaka, W. Cai, K. Suita, R. Prajapati, C. Liang, Y.  
682 Ohnuki, Y. Mototani, M. Umemura, U. Yokoyama, M. Sato, S. Okumura, Y. Ishikawa, Epac  
683 activation inhibits IL-6-induced cardiac myocyte dysfunction, *J. Physiol. Sci.* 68 (2018) 77–  
684 87. <https://doi.org/10.1007/s12576-016-0509-5>.
- 685 [39] T.T. Sio, K. Chang, R. Jayakrishnan, D. Wu, M. Politi, D. Malacarne, J. Saletnik, M. Chung,  
686 Patient age is related to decision-making, treatment selection, and perceived quality of  
687 life in breast cancer survivors, *World J. Surg. Oncol.* 12 (2014) 230.  
688 <https://doi.org/10.1186/1477-7819-12-230>.
- 689 [40] S.D. Targum, R. Risinger, Y. Du, J.C. Pendergrass, H.H. Jamal, Bernard.L. Silverman, Effect  
690 of patient age on treatment response in a study of the acute exacerbation of psychosis  
691 in schizophrenia, *Schizophr. Res.* 179 (2017) 64–69.  
692 <https://doi.org/10.1016/j.schres.2016.09.034>.
- 693 [41] G. Basara, S.G. Ozcebe, B.W. Ellis, P. Zorlutuna, Tunable Human Myocardium Derived  
694 Decellularized Extracellular Matrix for 3D Bioprinting and Cardiac Tissue Engineering,  
695 *Gels*. 7 (2021) 70. <https://doi.org/10.3390/gels7020070>.
- 696 [42] X. Lian, J. Zhang, S.M. Azarin, K. Zhu, L.B. Hazeltine, X. Bao, C. Hsiao, T.J. Kamp, S.P.  
697 Palecek, Directed cardiomyocyte differentiation from human pluripotent stem cells by  
698 modulating Wnt/ $\beta$ -catenin signaling under fully defined conditions, *Nat. Protoc.* 8 (2013)  
699 162–175. <https://doi.org/10.1038/nprot.2012.150>.
- 700 [43] J.F. Murphy, J. Mayourian, F. Stillitano, S. Munawar, K.M. Broughton, E. Agullo-Pascual,  
701 M.A. Sussman, R.J. Hajjar, K.D. Costa, I.C. Turnbull, Adult human cardiac stem cell  
702 supplementation effectively increases contractile function and maturation in human  
703 engineered cardiac tissues, *Stem Cell Res. Ther.* 10 (2019) 373.  
704 <https://doi.org/10.1186/s13287-019-1486-4>.
- 705 [44] Z. Xie, A. Bailey, M.V. Kuleshov, D.J.B. Clarke, J.E. Evangelista, S.L. Jenkins, A. Lachmann,  
706 M.L. Wojciechowicz, E. Kropiwnicki, K.M. Jagodnik, M. Jeon, A. Ma'ayan, Gene Set  
707 Knowledge Discovery with Enrichr, *Curr. Protoc.* 1 (2021) e90.  
708 <https://doi.org/10.1002/cpz1.90>.
- 709 [45] W. Liebermeister, E. Noor, A. Flamholz, D. Davidi, J. Bernhardt, R. Milo, Visual account of  
710 protein investment in cellular functions, *Proc. Natl. Acad. Sci. U. S. A.* 111 (2014) 8488–  
711 8493. <https://doi.org/10.1073/pnas.1314810111>.
- 712